ACS APPLIED MATERIALS & INTERFACES

Research Article

www.acsami.org

Layered Double Hydroxide–Carbon Dot Composite: High-Performance Adsorbent for Removal of Anionic Organic Dye

Manlin Zhang,[†,§] Qingfeng Yao,[†,§] Chao Lu,*[,†] Zenghe Li,*[,†] and Wenxing Wang[‡]

[†]State Key Laboratory of Chemical Resource Engineering, Beijing University of Chemical Technology, Beijing 100029, China

[‡]Chinese Research Academy of Environmental Sciences, Beijing 100012, China

Supporting Information

ABSTRACT: It would be of significance to design a green composite for efficient removal of contaminants. Herein, we fabricated a facile and environmentally friendly composite via direct assembly of surface passivated carbon dots with abundant oxygen-containing functional groups on the surface of the positively charged layered double hydroxide (LDH). The resulting LDH–carbon dot composites were characterized by X-ray diffraction (XRD), Fourier transformed infrared (FTIR) spectroscopy, high resolution transmission electron microscopy (HRTEM), scanning electron microscopy (SEM), and N_2 adsorption–desorption technique. The adsorption performances of the resulting LDH–carbon dot composites were evaluated for the removal of anionic methyl blue dye. Taking advantage of the combined benefits of LDH and carbon dots, the as-prepared composites exhibited high uptake capability of methyl blue (185 mg/g). The adsorption behavior of this new adsorbent fitted well with Langmuir isotherm and the pseudo-second-order kinetic model. The reasons for the excellent adsorption capacity of methyl blue on the surface of the LDH–carbon dot hybrid were further discussed. A probable mechanism was speculated to involve the cooperative contributions of hydrogen bonding between methyl blue and carbon dots and electrostatic attraction between methyl blue and LDH, in the adsorption process. This work is anticipated to open up new possibilities in fabricating LDH–carbon dot materials in dealing with anionic dye pollutants.

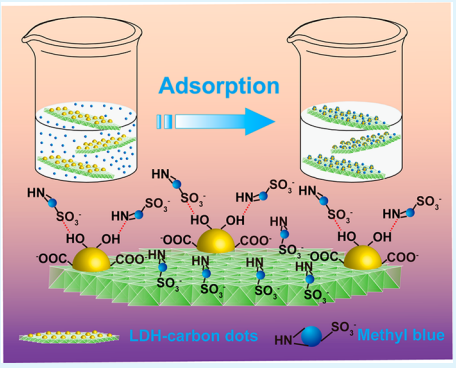

KEYWORDS: *layered double hydroxides, carbon dots, electrostatic attraction, anionic organic dye*

1. INTRODUCTION

Surface passivated carbon dots contain abundant oxygen-containing functional groups (−OH, −COOH, and −C═O) on the surface of carbon dots.[1−3] Considering these oxygen-containing functional groups, easy preparation, high surface area, and low toxicity,[4] carbon dots should be promising to turn into an alternative material for removal of a variety of organic and inorganic contaminants. However, to our knowledge, no report has addressed this topic due to high solubility of carbon dots. To resolve this problem, Kang and his coauthors employed gold nanoparticles as supports to fabricate a carbon dot–gold nanoparticle composite for nitroaromatic adsorption as a result of the formation of hydrogen bonding between the hydroxyl groups on the surface of carbon dots and nitroaromatic.[5] However, such the hydrogen bonding interactions were relatively weak. Therefore, it is still indispensable to exploit a novel carbon dot-based adsorbent material for the improvement on the adsorption efficiency using other supports exhibiting the cooperative contributions to the adsorption behavior of carbon dots.

Layered double hydroxide (LDH) is important inorganic layered materials with the general formula $[M_{1-x}^{II}M_x^{III}(OH)_2]^{x+}$ $(A^{n-})_{x/n}\cdot mH_2O$, where M^{II} and M^{III} are divalent and trivalent metal ions in the octahedral positions of brucite-like layers with excessive positive charge and A^{n-} represents a nonframework inorganic or organic n-valent anion compensating the interlayer anions related to hydrotalcite.[6−8] The inherent structure feature allows LDH to become promising adsorbents to capture a range of anionic pollutants in aqueous solutions.[9−12] In general, three different mechanisms of LDH have been proposed to control the removal of contaminants from aqueous solutions, namely electrostatic attraction,[13,14] ion exchange,[15−17] and van der Waals force.[18] In addition, hydrogen bonding interactions are formed between hydroxyl groups of LDH and the nitrogen or oxygen-containing groups from adsorbates.[19−21] However, these hydrogen bonding interactions play a limited role in the adsorption process due to the fact that only the free hydroxyl groups in the brucite-like sheets can serve as the binding sites for oxygen/nitrogen-containing groups.[21] Therefore, we are interested in fabricating tailored functional composite-based LDH in order to enhance the adsorption sites of LDH for hydrogen bonding.

Utilizing a strategy of fabricating composites by assembling the positively charged LDH and carbon dots with abundant oxygen-containing functional groups for the removal of

Received: August 26, 2014
Accepted: October 14, 2014
Published: October 14, 2014

contaminants would be of significance. However, to the best of our knowledge, there is no report on the application of LDH−carbon dot composites as versatile adsorbents. In this study, we fabricated a facile assembly via direct assembly of carbon dots on the surface of LDH. The resulting LDH−carbon dot composites were characterized by X-ray diffraction (XRD), Fourier transformed infrared (FTIR) spectroscopy, high resolution transmission electron microscopy (HRTEM), scanning electron microscopy (SEM), and N_2 adsorption−desorption technique. Furthermore, the adsorptive capacity of such a composite was evaluated by using methyl blue as a model anionic dye. In fact, there were lots of hydroxyl groups on the surface of LDH. However, only free hydroxyl groups in the LDH sheets can form hydrogen bonding.[21] In this work, it was observed that the introduction of carbon dots into the LDH can donate abundant hydroxyl groups on the surface of LDH, facilitating the formation of hydrogen bonding between carbon dots and methyl blue (Figure 1). Accordingly, the adsorption efficiency of the resulting assembly of LDH−carbon dot composite can be greatly improved as a result of the cooperative contributions of hydrogen bonding between methyl blue and carbon dots and electrostatic attraction between methyl blue and LDH.

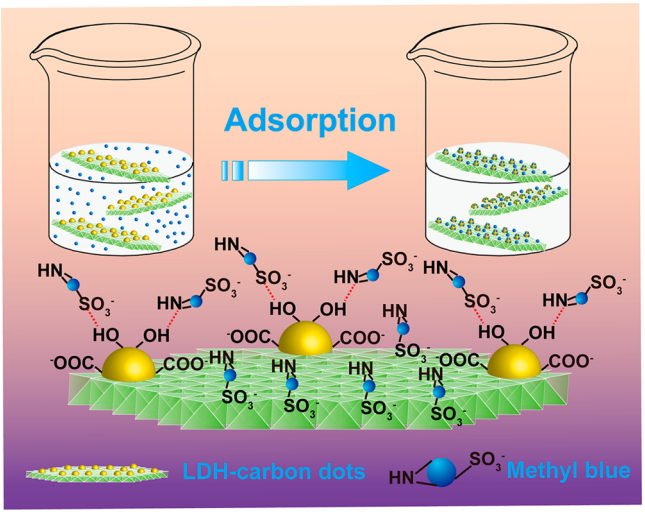

Figure 1. Schematic proposed view of methyl blue adsorption on LDH−carbon dot composites.

2. EXPERIMENTAL SECTION

2.1. Materials. All solutions were prepared with deionized water (Milli Q, Millipore, Barnstead, CA, USA). Methyl blue ($C_{37}H_{27}N_3O_9S_3{\cdot}Na_2$, > 99.7%), Rhodamine B ($C_{28}H_{31}N_2O_3{\cdot}Cl$, > 95.0%), and methyl orange ($C_{14}H_{14}N_3O_3S{\cdot}Na$, > 80.0%) were purchased from Tianjin Guangfu Fine Chemical Research Institute (Tianjin, China). $Mg(NO_3)_2{\cdot}6H_2O$, $Al(NO_3)_3{\cdot}9H_2O$, NaCl, Na_2SO_4, Na_2CO_3, Na_3PO_4, $NaNO_3$, NaOH, HCl, and glycerin were purchased from Beijing Chemical Reagent Company (Beijing, China). Poly(ethylene glycol) 1500 (PEG 1500) and serine were purchased from Sigma-Aldrich Chemical Co. (St. Louis, MO, USA). All reagents used in this study were analytical grade without further purification.

2.2. Apparatus. The powder XRD measurements were performed on a Bruker (Germany) D8 ADVANCE X-ray diffractometer equipped with graphite-monochromatized Cu Kα radiation (λ = 1.5406 Å). The 2θ angle of the diffractometer was stepped from 5° to 70° at a scan rate of 10°/min. FTIR spectra (resolution, 4.0 cm^{-1}; number of scans, 32) were recorded on a Nicolet 6700 FTIR spectrometer (Thermo, America). TEM images were obtained using a Tecnai G220 (FEI, Hong Kong) instrument. HRTEM images were obtained on a JEOL JEM-2100 transmission electron microscope. The morphology was studied using an S-4700 field-emission SEM instrument. N_2 adsorption−desorption isotherms were measured at 77 K using ASAP 2020 nitrogen adsorption apparatus (Micromeritics Ins. Corp., USA). Specific surface areas were calculated according to the Brunauer−Emmett−Teller (BET) equation from the linear part of the BET plot. The pore-size distributions of samples were calculated from desorption branch using the Barrett−Joyner−Halenda (BJH) method. The ζ-potentials of the fabricated LDH−carbon dot composite were determined on a Zetasizer 3000HS nanogranularity analyzer (Malvern Instruments, UK). UV−visible spectra were measured on a USB 4000 miniature fiber optic spectrometer in absorbance mode with a DH-2000 deuterium and tungsten halogen light source (Ocean Optics, Dunedin, FL). Fluorescence spectra were measured with a Hitachi F-7000 fluorescence spectrophotometer (Tokyo, Japan). An 800 W microwave oven (G8023CSL-K3, Galanz, China) was used for the preparation of carbon dots. The centrifugation was operated on a TGL-16B centrifugal machine (Shanghai Anting Scientific Instrument Factory, Shanghai, China).

2.3. Synthesis of Mg−Al−CO_3 LDH. Mg−Al−CO_3 LDH was synthesized according to the coprecipitation method as follows: 60 mL of salt solution containing 0.045 mol $Mg(NO_3)_2{\cdot}6H_2O$ and 0.015 mol $Al(NO_3)_3{\cdot}9H_2O$ and 60 mL of alkaline solution containing 0.12 mol NaOH and 0.01 mol Na_2CO_3 were added dropwise into a 250 mL four-necked flask under vigorous stirring. The pH value of the solution remained 10 in the synthesis process. After then, the mixture was stirred for 24 h at 333 K. Finally, the obtained precipitate was washed thoroughly with deionized water for three times and dried under vacuum for 24 h at 338 K.

2.4. Synthesis of Carbon Dots. Carbon dots were synthesized by a microwave method. 1.0 g of PEG 1500 was dissolved in 15 mL of glycerin and then the homogeneous solution was heated for 1 min in a microwave oven. After that, 0.5 g of serine was added in this solution. Finally, this mixture was further heated in a microwave oven for another 6 min. The solution changed from colorless to dark brown over the reaction. The resulting solution kept stable for several months in a refrigerator at 282 K.

2.5. Fabrication of LDH−Carbon Dot Composites. LDH−carbon dot composites were prepared by the colloidal deposition method. The 150 mg CO_3−LDH support was added to the 5.0 mL carbon dot colloidal solution under vigorous stirring and kept in contact for 60 min at room temperature. The obtained precipitate after centrifugation was washed thoroughly with deionized water for three times and then dried under vacuum at 333 K overnight.

2.6. Adsorption Experiments. Adsorption experiments were carried out by agitating the 10 mg LDH−carbon dot composite adsorbent (pH 9.45) with a series of methyl blue solutions from 40 to 160 mg/L (20 mL). The adsorption experiment of carbon dots was implemented by a dialysis method (MWCO 1000 semipermeable membrane) using methyl blue solution as the dialysate. The adsorption effects were monitored by taking 2 mL sample solutions at 5 min time intervals (from 5 to 90 min) during the adsorption process and the equilibrium time was 60 min. The residual methyl blue concentration in the sample solution was analyzed using the UV−visible spectrophotometer at 627 nm after the LDH−carbon dot powder was separated by centrifugation (10000 rpm/min, 3 min). The percentage removal of methyl blue from the solution was calculated by $(C_0 - C_e)/C_0 \times 100\%$, and the amount of methyl blue adsorbed at equilibrium q_e (mg/g) was calculated by $q_e = (C_0 - C_e) \times V/W$, where C_0 and C_e are the initial and equilibrium concentrations of adsorbate solution (mg/L), V denotes the volume of methyl blue solution used (L), and W is the mass in grams of the adsorbent used. The results shown here were the mean of three determinations.

3. RESULTS AND DISCUSSION

3.1. Characterization of LDH−Carbon Dot Composites. The precursors of LDH−carbon dot composites, namely

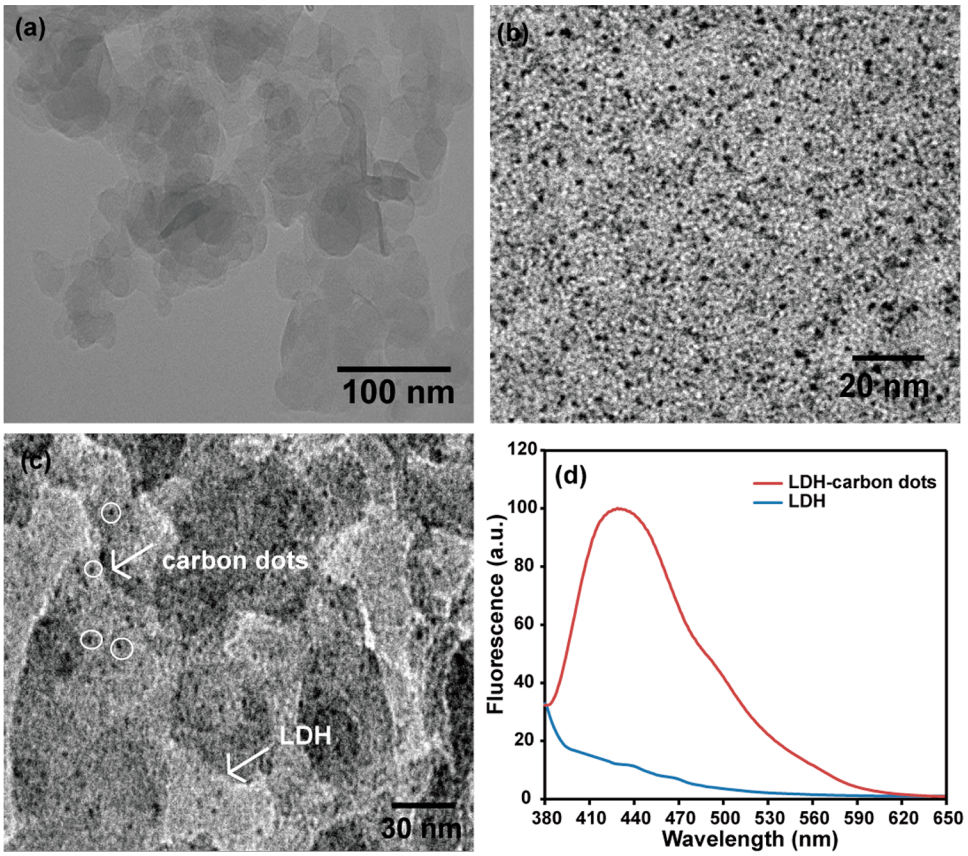

Figure 2. TEM image of LDH (a), HRTEM images of carbon dots (b), LDH−carbon dots (c); normalized fluorescence spectra of LDH and LDH−carbon dots (λ_{ex} = 360 nm) (d).

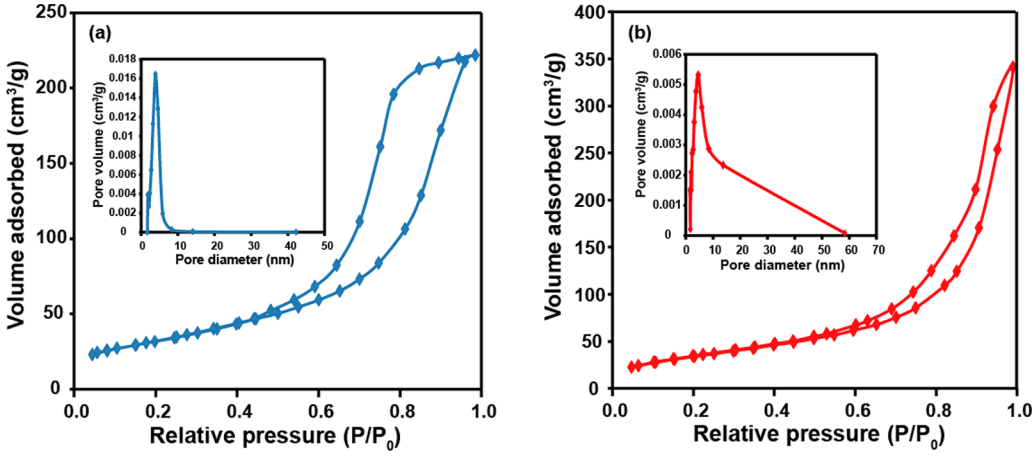

Figure 3. N_2 adsorption−desorption isotherms and pore size distributions of (a) LDH and (b) LDH−carbon dots.

CO_3−LDH and carbon dots, were synthesized. The XRD pattern for the CO_3−LDH displayed narrow, symmetric, and strong diffraction peaks at low 2θ values (5° to 25°) and weaker and less symmetric diffraction peaks at high 2θ values (25° to 70°) (Figure S1a, Supporting Information).[22] The XRD pattern for the carbon dots was presented in Figure S1b, Supporting Information, it was a broad peak near 21° with a relatively low intensity. This phenomenon was attributed to amorphous carbon.[23] In addition, the TEM image of the as-prepared CO_3−LDH showed a platelet structure (Figure 2a). The HRTEM image of the synthesized carbon dots demonstrated about 5 nm spherical particles with a narrow size distribution (Figure 2b). In addition, the fluorescence spectra of the carbon dots described the strongest emission peak at 410 nm for excitation at 330 nm (Figure S2, Supporting Information). CO_3−LDH is the most stable in all LDH because it has a particularly high affinity between carbonate and the layer region of LDH.[24] As a result, CO_3-LDH crystals cannot be broken by vigorous stirring, and other anions cannot replace carbonate ions by anionic exchange. In addition, the surface charges of LDH, carbon dots, and LDH−carbon dot composites were +26.7, −4.3, and +23.1 mV, respectively. Therefore, carbon dots can be attached on the surface of CO_3−LDH by electrostatic attraction.

The HRTEM image of the fabricated LDH−carbon dot composites clearly indicated that the carbon dots were assembled on the surface of the LDH effectively and dispersedly (Figure 2c), which can be further confirmed by comparing fluorescence intensity of the LDH−carbon dots and the raw LDH (Figure 2d).

The FTIR spectra of CO_3−LDH and LDH−carbon dots are shown in Figure S3, Supporting Information. The characteristic adsorption bands at 3486 and 1646 cm^{-1} were attributed to the hydroxyl groups of the interlayered water molecules. The adsorption band at 1373 cm^{-1} was the asymmetric stretching vibration mode of C−O in carbonate and the band at 659 cm^{-1} was assigned to the metal−oxygen−metal stretching.[18] In comparison, the FTIR spectrum of LDH−carbon dots showed that there appeared a new adsorption band at around 1010 cm^{-1} corresponded to the bending vibrations of C−O−C of carbon dots (Figure S4, Supporting Information),[25] indicating that the carbon dots had been successfully loaded on the LDH.

The surface properties of the LDH and LDH−carbon dot composites were investigated using N_2 adsorption−desorption measurements. The N_2 adsorption−desorption isotherms and the corresponding BJH pore size distribution plots for the LDH and LDH−carbon dots were displayed in Figure 3. The adsorption−desorption isotherm of LDH exhibited a type IV with H2 hysteresis loop, characteristic of mesoporous materials with regular pore size distribution.[26] The pore structure of LDH was basically mesoporous with a narrow unimodal pore size distribution centered at 3.92 nm (inset of Figure 3), which was correlated to the aggregation of LDH flake-like particles.[16] In contrast, the LDH−carbon dot composites were related to type IV with H3-type hysteresis loop. Furthermore, limiting adsorption did not appear at high p/p_0 region, suggesting the presence of mesopores and macropores.[27] The pore size distribution curve of the LDH−carbon dots was broad with mesopores and macropores. The formed macropores reflected the numerous gaps between the carbon dots.[28] Finally, the calculated data of specific surface area, total pore volume, and average pore width for the LDH and LDH−carbon dots are inspected in Table S1, Supporting Information. It was obvious that the structural parameters of the LDH−carbon dot composites were larger than those of the raw LDH.

3.2. Highly Efficient Adsorption of Methyl Blue on LDH−Carbon Dot Composites. The adsorption activities of carbon dots, LDH, and LDH−carbon dots toward methyl blue were compared as a function of time under continuous stirring at room temperature. As shown in Figure 4, 96% of 80 mg/L methyl blue was adsorbed on the surface of the LDH−carbon dot composites within 20 min. However, the raw LDH can only adsorb 45% methyl blue under the same conditions. Note that no uptake was observed in the presence of carbon dots. These interesting results demonstrated that the LDH−carbon dot composites displayed higher adsorption activities than carbon dots or LDH, indicating that the attachment of carbon dots on the surface of the LDH facilitated the formation of hydrogen bonding between carbon dots and methyl blue.

3.3. Adsorption Isotherms. In general, adsorption isotherms are carried out to give qualitative information on the adsorption capacity of adsorbents and the distribution of adsorbates between liquid phase and solid phase when the adsorption process reaches equilibrium.[29] As shown in Figure 5, the adsorbed amount of methyl blue increased with an increase in the equilibrium concentrations of methyl blue upon 12 mg/L. The maximum adsorption capacity in the uptake of

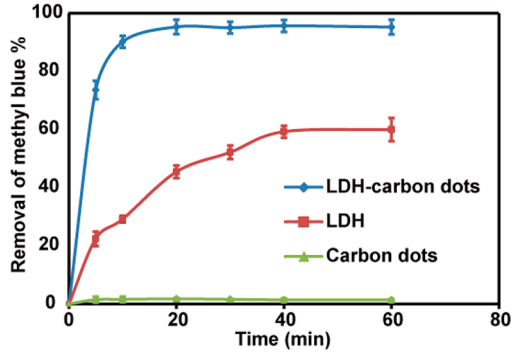

Figure 4. Percentage removal of methyl blue from an aqueous solution over different adsorbents including carbon dots, LDH, and LDH−carbon dots (80 mg/L methyl blue, 0.5 g/L adsorbent dose, T = 298 K).

methyl blue from aqueous solutions achieved about 185 mg/g, which has been compared with the reported adsorbent (Table S2, Supporting Information).[30−32] In addition, the color of adsorbent before and after the removal of methyl blue changed from bright yellow to dark blue (inset of Figure 5a). The equilibrium adsorption data were analyzed by well-known Langmuir ($C_e/q_e = 1/bq_m + C_e/q_m$), Freundlich ($\log q_e = \log k_f + 1/n \log C_e$), and Dubinin−Radushkevich (D−R) ($\ln q_e = \ln q_m - \beta\varepsilon^2$) isotherm models,[33−35] where C_e (mg/L) is the adsorbate concentration in the equilibrium solution, q_e (mg/g) is the equilibrium amount of adsorbate on the adsorbent, b (L/mg) is the Langmuir constant related to the adsorption energy, q_m (mg/g) is the maximum adsorption capacity of the adsorbent corresponding to the complete monolayer coverage, k_f and $1/n$ are Freundlich constants related to adsorption capacity and adsorption intensity, β (mol^2/kJ^2) is the D−R isotherm constant related to the free energy of adsorption, and ε is the Polanyi potential ($\varepsilon = RT \ln (1 + 1/C_e)$). A dimensionless constant known as separation factor (R_L) can be represented as $R_L = 1/(1 + bC_0)$. The R_L value was used to predict the adsorption nature to be either irreversible ($R_L = 0$), favorable ($0 < R_L < 1$), linear ($R_L = 1$), or unfavorable ($R_L > 1$). The calculated R_L values are between 0 and 1 at different initial concentrations of methyl blue, indicating that the adsorption of methyl blue on the LDH−carbon dots is favorable.[36] On the other hand, the $1/n$ for LDH−carbon dots was 0.20, further confirming highly efficient adsorption capacity of methyl blue on LDH−carbon dots. The D−R model is usually used to distinguish the physical and chemical adsorption by calculating its mean free energy of adsorption (E, kJ/mol) as follows: $E = (1/2\ \beta)^{1/2}$. In this system, the E of methyl blue adsorption was 1.0 kJ/mol, indicating that adsorption process of methyl blue on the LDH−carbon dot composites was carried out by physical adsorption.[35]

The isotherm data obtained were fitted by three isotherm models (Figure 5b,d). It was observed that the value of correlation coefficient (R^2) for Langmuir model was higher than those of other two models (Table S3, Supporting Information). The equilibrium adsorption capacity calculated by the Langmuir model was consistent with that obtained by experiments, meaning that the adsorption isotherm of methyl blue on the LDH−carbon dots was suitable for Langmuir model. These results demonstrated that the surface of LDH−carbon dots was homogeneous with the adsorption mechanism of monolayer uptake.[37,38]

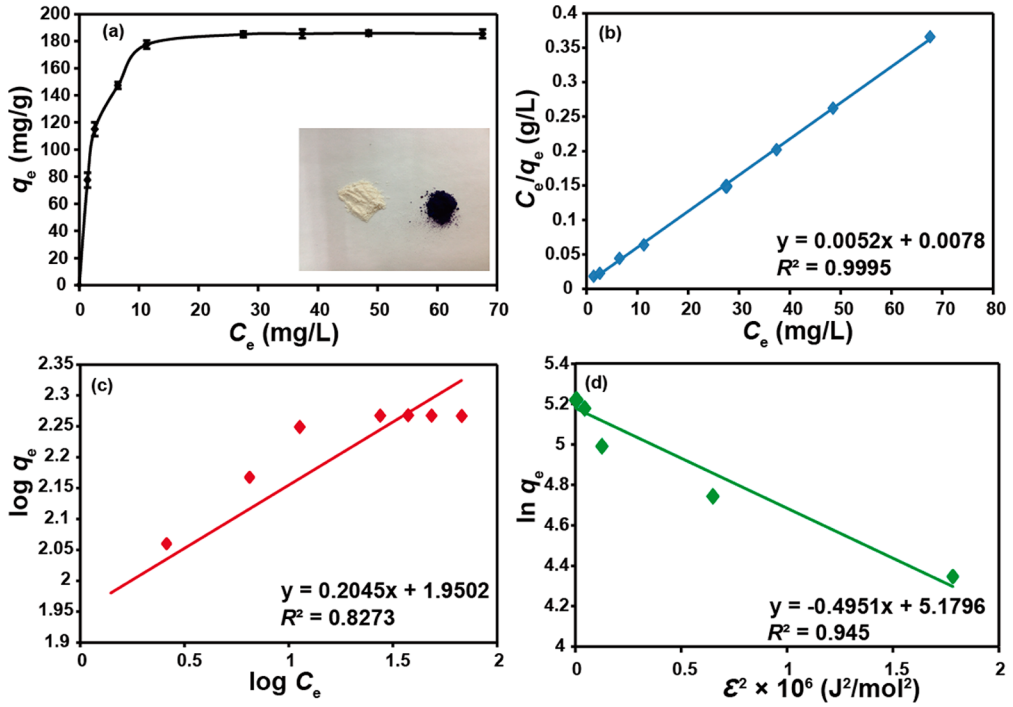

Figure 5. (a) Adsorption isotherm of methyl blue on the surface of LDH−carbon dots (inset: the LDH−carbon dot powder before (left) and after (right) adsorbing methyl blue, (b) Langmuir isotherm model, (c) Freundlich isotherm model, and (d) D−R isotherm model (0.5 g/L adsorbent dose, T = 298 K).

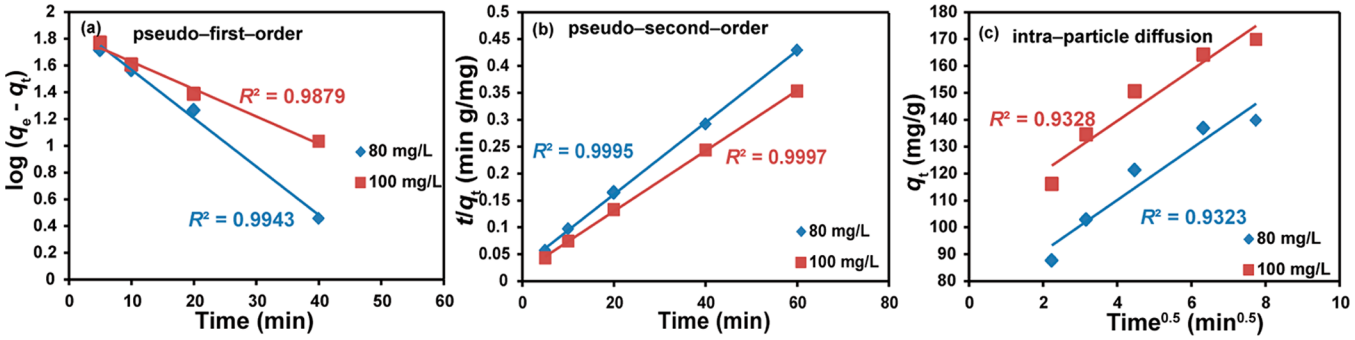

Figure 6. Plots of (a) pseudo-first-order kinetics, (b) pseudo-second-order kinetics, and (c) intraparticle diffusion models of methyl blue on the surface of LDH−carbon dots (0.5 g/L adsorbent dose, T = 298 K).

3.4. Adsorption Kinetics. To investigate the adsorption rate and the mechanism of adsorption process, kinetics of methyl blue adsorption on LDH−carbon dots were analyzed using the pseudo-first-order ($\log (q_e - q_t) = \log q_e - k_1 \times t/2.303$),[39] the pseudo-second-order ($t/q_t = 1/k_2 q_e^2 + t/q_e$),[40] and intraparticle diffusion kinetic models ($q_t = k_i t^{0.5} + C$),[37] respectively, where q_t (mg/g) and q_e (mg/g) represent the amount of methyl blue adsorbed at time t and at equilibrium time, respectively, k_1 (min^{-1}), k_2 (g/mg·min), and k_i (mg/g·min$^{0.5}$) represent the rate constant of the pseudo-first-order model, the pseudo-second-order model, and the intraparticle diffusion model, respectively, C is the intercept.

Under the optimum dosage of the LDH−carbon dots (Figure S5, Supporting Information), 80 and 100 mg/L (Figure S6, Supporting Information) were selected as the two initial methyl blue concentrations to study the adsorption kinetics. From Figure 6, and Table S4, Supporting Information, we found that the pseudo-second-order model can best describe the kinetic data for methyl blue adsorption on the surface of the LDH−carbon dots because it possessed a higher R^2 value. These results indicated that the rate-limiting step in the present system was chemical adsorption.[41]

3.5. Possible Adsorption Mechanism of Methyl Blue with LDH−Carbon Dots. The efficient uptake mechanism of methyl blue by the assembly was investigated to clarify the adsorption process. UV−vis spectra of methyl blue before and after adsorption are shown in Figure 7a; it was obvious that the characteristic adsorption peak of methyl blue disappeared after adsorption. Note that the initial pH value of methyl blue was 7.38. Therefore, before and after the adsorption, we did not adjust the pH of the methyl blue solution as a result of the strong buffering capacity of the LDH−carbon dot composites.[42] The corresponding photographs displayed that the color of methyl blue solution was changed from deep blue to the clean and colorless solution after adsorption (see inset of Figure 7a). This phenomenon indicated that the methyl blue molecules could be efficiently adsorbed on the surface of LDH−carbon dot composites. To further investigate the

dx.doi.org/10.1021/am505765e | ACS Appl. Mater. Interfaces 2014, 6, 20225−20233

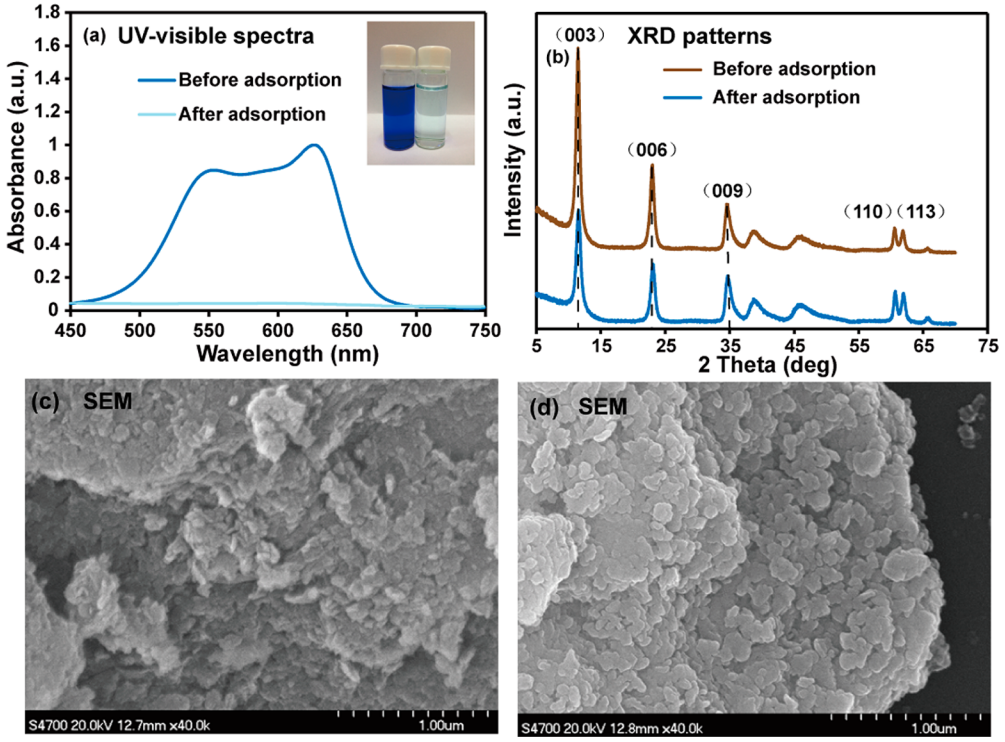

Figure 7. (a) UV−visible spectra of methyl blue before and after adsorption on the LDH−carbon dots (inset: photographs of methyl blue solution before and after adsorption), (b) XRD patterns of LDH−carbon dots before and after adsorption of methyl blue, (c) SEM images of LDH−carbon dots after adsorption of methyl blue, and (d) SEM images of LDH−carbon dots before adsorption of methyl blue (80 mg/L methyl blue, 0.5 g/L adsorbent dose, T = 298 K).

adsorption performance of LDH−carbon dots, it was applied in simulated dye wastewater containing methyl orange (anionic), Rhodamine B (cationic), and methyl blue (anionic) (Figure S7, Supporting Information). The results indicated that LDH−carbon dots had the ability to selectively adsorb anionic dyes from dye wastewater. Figure 7b shows that the XRD patterns of LDH−carbon dots before and after adsorption of methyl blue did not show any obvious changes, indicating that the structure of composites was preserved. The morphological features of the LDH−carbon dot composites before and after adsorption were characterized by SEM images. After adsorption, we clearly observed that the surface of the composite became rough and curly with a white layer on the surface (Figure 7c). Mechanical stirring may affect the morphological feature and surface characteristic of the LDH−carbon dot adsorbent. Therefore, the control experiment (in the absence of methyl blue) was carried out under the same experimental conditions, and the results showed that the surface of composite was smooth (Figure 7d). These findings demonstrated the abundant accumulation of methyl blue over the surface of LDH−carbon dots.[35]

The effects of competitive anions were studied by adding the mixture solution of 80 mg/L methyl blue and 0.01 mol/L sodium salt into the proposed adsorption system. The tested sodium salts included NaCl, $NaNO_3$, Na_2SO_4, Na_2CO_3, or Na_3PO_4, respectively. As shown in Figure S8, Supporting Information, the effect of monovalent anions on methyl blue uptake was negligible. On the contrary, the divalent and trivalent anions had a profound effect on the adsorption process, indicating the occurrence of the competition adsorption between methyl blue molecules and inorganic anions.[43] These interesting findings confirmed the existence of electrostatic interactions between methyl blue and LDH−carbon dot composites.

The adsorption capacity of methyl blue on the surface of LDH−carbon dots was affected by pH.[42] In this work, the pH values of methyl blue on the adsorption process was carried out from 2 to 12. From Figure S9a, Supporting Information, we could see that the percentage of adsorption kept constant in the pH range of 4−10, and decreased with further fluctuations in the pH values. Generally, acidic conditions contribute to the formation of hydrogen bonding; however, the lower pH values (pH < 4) may induce the destruction of the LDH layered structure. In addition, the competition effects between excess OH^- ions and methyl blue in the higher pH (pH > 10) also affected the adsorption performance.[16] Furthermore, the occurrence of deprotonation could reduce the positive charge on the surface of LDH−carbon dots, leading to worse adsorption capacity (Figure S9b, Supporting Information).

The relationship between the initial and equilibrium pH values was also shown in Figure S9a, Supporting Information. The equilibrium pH remained constant in the range of 4 to 10 due to a buffering capacity of the LDH−carbon dot composites.[42] Note that the general pH value in dye wastewater is 6−9. Therefore, the fabricated LDH−carbon dot composites are suitable for wastewater treatment in textile industry without the need of preliminary pH adjustment.

Figure 8 compares the FTIR spectra of LDH and LDH−carbon dots after adsorption of methyl blue, respectively. For LDH and LDH−carbon dots, the peaks appeared at 1183 and 1038 cm^{-1} associated with the asymmetric and symmetric stretching vibrations of the $-SO_3^-$ group.[20] Those findings indicated that methyl blue molecules can be successfully absorbed on the surface of the LDH and LDH−carbon dots,

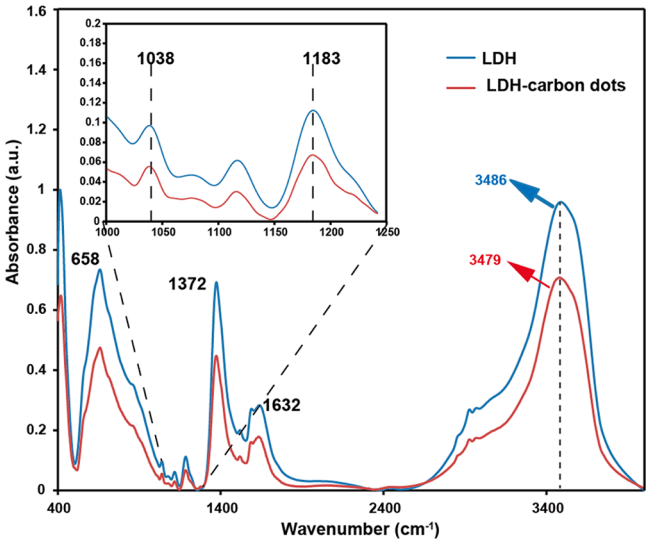

Figure 8. FTIR spectra of the LDH and LDH−carbon dots after adsorption of methyl blue.

respectively. Furthermore, the characteristic peak of hydroxyl group of LDH−carbon dots shifted from 3490 to 3479 cm^{-1} (blue shifted). However, the characteristic peak of hydroxyl group of LDH did not have an obvious change. These results indicated the formation of more hydrogen bonding between hydrogen atom of the free hydroxyl groups of carbon dots and nitrogen or oxygen-containing groups of methyl blue in the adsorption process.[44,45] In addition, Figure S10, Supporting Information, shows that the adsorption capacity of LDH−carbon dots was decreased by increasing adsorption temperature from 308 to 323 K, due to the sensitivity of the length and strength of hydrogen bonding toward temperature.[46−48] In addition, in order to further confirm the formation of hydrogen bonding between LDH−carbon dots and methyl blue, we evaluated the adsorption enthalpy (ΔH).[49] Adsorption isotherm for methyl blue on the surface of LDH−carbon dots at different temperature are shown in Figures 5A and S10, Supporting Information. The ΔH was calculated by the van't Hoff method ($\ln b = \Delta S/R - \Delta H/RT$), where ΔH is change in enthalpy (J/mol), ΔS is the change in entropy (J/(mol K)), R is the universal gas constant (8.314 J/K mol), and b is the Langmuir constant at temperature T (K). The van't Hoff polt and ΔH for adsorption of methyl blue on the LDH−carbon dots are shown in Figure S11 and Table S5, Supporting Information. The ΔH of the adsorption was −12.2 kJ/mol, in the range of the hydrogen bonding force (0 ∼ −20 kJ/mol),[50] indicating that the hydrogen bonding took an important role in adsorption process.

In conclusion, methyl blue can be adsorbed on the LDH−carbon dot composites by electrostatic attraction between methyl blue and LDH. In addition, the carbon dots attached on the surface of LDH facilitated the formation of hydrogen bonding between carbon dots and methyl blue. However, in the absence of LDH, the hydrogen bonding interaction between carbon dots and methyl blue may be suppressed due to the electrostatic repulsion between carbon dots and methyl blue. Therefore, the cooperative contribution of hydrogen bonding between methyl blue and carbon dots and electrostatic attraction between methyl blue and LDH is beneficial to the improvement of adsorption capacity.

4. CONCLUSIONS

In summary, the LDH−carbon dot composites were successfully synthesized via direct assembly of carbon dots on the surface of LDH. The resulting LDH−carbon dots showed excellent adsorption ability to methyl blue, owing to the cooperative contributions of hydrogen bonding and electrostatic attraction between methyl blue and composites. The adsorption isotherm of methyl blue on the surface of the LDH−carbon dots was suitable for the Langmuir model, indicative of a monolayer adsorption. The adsorption kinetic followed the pseudo-second-order kinetic model. Our findings provide a new insight into designing effective composite-based LDH for improving the adsorption capacity of methyl blue. As a promising adsorbent for anion dyes, the LDH−carbon dot hybrid may be a promising candidate to remove anionic pollutants from aqueous solutions in environmental pollution management in the near future.

■ ASSOCIATED CONTENT

Ⓢ Supporting Information

XRD patterns of CO_3−LDH, and carbon dots; fluorescence spectra at different excitation wavelengths of the carbon dots; FTIR spectra of the LDH and LDH−carbon dots; effects of adsorbent dosage, time, initial concentration, competitive anions, pH, and temperature on removal of methyl blue; ζ-potential of LDH−carbon dots as a function of pH; UV−visible spectra of simulated dye wastewater before and after adsorption on the LDH−carbon dots; van't Hoff polt for adsorption of methyl blue on the LDH−carbon dots; structural parameters of raw LDH and LDH−carbon dots; maximum adsorption capacities for the adsorption of methyl blue onto various adsorbents; Langmuir, Freundlich, and D−R isotherm parameters of LDH−carbon dots; parameters of kinetic models for the adsorption of methyl blue on LDH−carbon dots; adsorption enthalpies ΔH (kJ/mol) for the adsorption of methyl blue on LDH−carbon dots. This material is available free of charge via the Internet at http://pubs.acs.org.

■ AUTHOR INFORMATION

Corresponding Authors

*C. Lu. E-mail: luchao@mail.buct.edu.cn. Fax/Tel.: +86 10 64411957.

*Z. Li. E-mail: lizh@mial.buct.edu.cn. Fax/Tel.: +86 10 64411957.

Author Contributions

§M. Zhang and Q. Yao contributed equally to this work.

Notes

The authors declare no competing financial interest.

■ ACKNOWLEDGMENTS

This work was supported by National Basic Research Program of China (973 Program, 2014CB932103), the National Natural Foundation of China (21375006), the 973 Program (2011CBA00503), and the Fundamental Research Funds for the Central Universities (JD1311). We also thank Prof. Xue Duan, Beijing University of Chemical Technology, for his valuable discussions.

■ REFERENCES

(1) Ding, C. Q.; Zhu, A. W.; Tian, Y. Functional Surface Engineering of C-Dots for Fluorescent Biosensing and in Vivo Bioimaging. *Acc. Chem. Res.* **2014**, *47*, 20−30.

(2) Wu, L. N.; Luderer, M.; Yang, X. X.; Swain, C.; Zhang, H. Y.; Nelson, K.; Stacy, A. J.; Shen, B. Z.; Lanza, G. M.; Pan, D. Surface Passivation of Carbon Nanoparticles with Branched Macromolecules Influences Near Infrared Bioimaging. *Theranostics* **2013**, *3*, 677−686.
(3) Cao, L.; Wang, X.; Meziani, M. J.; Lu, F. S.; Wang, H. F.; Luo, P. G.; Lin, Y.; Harruff, B. A.; Veca, L. M.; Murray, D.; Xie, S.-Y.; Sun, Y.-P. Carbon Dots for Multiphoton Bioimaging. *J. Am. Chem. Soc.* **2007**, *129*, 11318−11319.
(4) Baker, S. N.; Baker, G. A. Luminescent Carbon Nanodots: Emergent Nanolights. *Angew. Chem., Int. Ed.* **2010**, *49*, 6726−6744.
(5) Liu, R. H.; Liu, J.; Kong, W. Q.; Huang, H.; Han, X.; Zhang, X.; Liu, Y.; Kang, Z. H. Adsorption Dominant Catalytic Activity of a Carbon Dots Stabilized Gold Nanoparticles System. *Dalton Trans.* **2014**, *43*, 10920−10929.
(6) Tang, D.; Liu, J.; Wu, X. Y.; Liu, R. H.; Han, X.; Han, Y. Z.; Huang, H.; Liu, Y.; Kang, Z. H. Carbon Quantum Dot/NiFe Layered Double-Hydroxide Composite as a Highly Efficient Electrocatalyst for Water Oxidation. *ACS Appl. Mater. Interfaces* **2014**, *6*, 7918−7925.
(7) Zhang, M. L.; Yao, Q. F.; Guan, W. J.; Lu, C.; Lin, J.-M. Layered Double Hydroxide-Supported Carbon Dots as an Efficient Heterogeneous Fenton-like Catalyst for Generation of Hydroxyl Radicals. *J.Phys. Chem. C* **2014**, *118*, 10441−10447.
(8) Wang, Y. L.; Wang, Z. C.; Rui, Y. P.; Li, M. G. Horseradish Peroxidase Immobilization on Carbon Nanodots/CoFe Layered Double Hydroxides: Direct Electrochemistry and Hydrogen Peroxide Sensing. *Biosens. Bioelectron.* **2015**, *64*, 57−62.
(9) Zhou, J. Z.; Wu, Y. Y.; Liu, C.; Orpe, A.; Liu, Q.; Xu, Z. P.; Qian, G. R.; Qiao, S. Z. Effective Self−Purification of Polynary Metal Electroplating Wastewaters through Formation of Layered Double Hydroxides. *Environ. Sci. Technol.* **2010**, *44*, 8884−8890.
(10) Wen, T.; Wu, X. L.; Tan, X. L.; Wang, X. K.; Xu, A. W. One-Pot Synthesis of Water-Swellable Mg−Al Layered Double Hydroxides and Graphene Oxide Nanocomposites for Efficient Removal of As (V) from Aqueous Solutions. *ACS Appl. Mater. Interfaces* **2013**, *5*, 3304−3311.
(11) Goh, K.-H.; Lim, T.-T.; Dong, Z. L. Enhanced Arsenic Removal by Hydrothermally Treated Nanocrystalline Mg/Al Layered Double Hydroxide with Nitrate Intercalation. *Environ. Sci. Technol.* **2009**, *43*, 2537−2543.
(12) Benselka-Hadj Abdelkader, N.; Bentouami, A.; Derriche, Z.; Bettahar, N.; de Ménorval, L.-C. Synthesis and Characterization of Mg−Fe Layer Double Hydroxides and Its Application on Adsorption of Orange G from Aqueous Solution. *Chem. Eng. J.* **2011**, *169*, 231−238.
(13) Saiah, F. B. D.; Su, B.-L.; Bettahar, N. Removal of Evans Blue by Using Nickel−Iron Layered Double Hydroxide (LDH) Nanoparticles: Effect of Hydrothermal Treatment Temperature on Textural Properties and Dye Adsorption. *Macromol. Symp.* **2008**, *273*, 125−134.
(14) Mustapha Bouhent, M.; Derriche, Z.; Denoyel, R.; Prevot, V.; Forano, C. Thermodynamical and Structural Insights of Orange II Adsorption by Mg_RAlNO_3 Layered Double Hydroxides. *J. Solid State Chem.* **2011**, *184*, 1016−1024.
(15) Drici Setti, N.; Jouini, N.; Derriche, Z. Sorption Study of an Anionic Dye-Benzopurpurine 4B-on Calcined and Uncalcined Mg-Al Layered Double Hydroxides. *J. Phys. Chem. Solids* **2010**, *71*, 556−559.
(16) Zaghouane-Boudiaf, H.; Boutahala, M.; Arab, L. Removal of Methyl Orange from Aqueous Solution by Uncalcined and Calcined MgNiAl Layered Double Hydroxides (LDHs). *Chem. Eng. J.* **2012**, *187*, 142−149.
(17) El Gaini, L.; Lakraimi, M.; Sebbar, E.; Meghea, A.; Bakasse, M. Removal of Indigo Carmine Dye from Water to Mg−Al−CO_3−Calcined Layered Double Hydroxides. *J. Hazard. Mater.* **2009**, *161*, 627−632.
(18) Ahmed, I. M.; Gasser, M. S. Adsorption Study of Anionic Reactive Dye from Aqueous Solution to Mg−Fe−CO_3 Layered Double Hydroxide (LDH). *Appl. Surf. Sci.* **2012**, *259*, 650−656.
(19) Zhang, C.; Yang, S. G.; Chen, H. Z.; He, H.; Sun, C. Adsorption Behavior and Mechanism of Reactive Brilliant Red X-3B in Aqueous Solution over Three Kinds of Hydrotalcite-like LDHs. *Appl. Surf. Sci.* **2014**, *301*, 329−337.
(20) de Sá, F. P.; Cunha, B. N.; Nunes, L. M. Effect of pH on the Adsorption of Sunset Yellow FCF Food Dye into a Layered Double Hydroxide (CaAl−LDH−NO_3). *Chem. Eng. J.* **2013**, *215−216*, 122−127.
(21) Lin, Y. J.; Fang, Q. L.; Chen, B. L. Metal Composition of Layered Double Hydroxides (LDHs) Regulating ClO^-_4 Adsorption to Calcined LDHs via the Memory Effect and Hydrogen Bonding. *J. Environ. Sci.* **2014**, *26*, 493−501.
(22) Gao, Y. S.; Wang, Q.; Wang, J. Y.; Huang, L.; Yan, X. R.; Zhang, X.; He, Q. L.; Xing, Z. P.; Guo, Z. H. Synthesis of Highly Efficient Flame Retardant High-Density Polyethylene Nanocomposites with Inorgano-Layered Double Hydroxides as Nanofiller Using Solvent Mixing Method. *ACS Appl. Mater. Interfaces* **2014**, *6*, 5094−5104.
(23) He, X. D.; Li, H. T.; Liu, Y.; Huang, H.; Kang, Z. H.; Lee, S.-T. Water Solution Carbon Nanoparticles: Hydrothermal Synthesis and Excellent Photoluminescence Properties. *Colloids Surf., B* **2011**, *87*, 326−332.
(24) He, S.; Zhao, Y. F.; Wei, M.; Duan, X. Preparation of Oriented Layered Double Hydroxide Film Using Electrophoretic Deposition and Its Application in Water Treatment. *Ind. Eng. Chem. Res.* **2011**, *50*, 2800−2806.
(25) Lin, Z.; Xue, W.; Chen, H.; Lin, J.-M. Peroxynitrous-Acid-Induced Chemiluminescence of Fluorescent Carbon Dots for Nitrite Sensing. *Anal. Chem.* **2011**, *83*, 8245−8251.
(26) Parida, K. M.; Mohapatra, L. Carbonate Intercalated Zn/Fe Layered Double Hydroxide: A Novel Photocatalyst for the Enhanced Photo Degradation of Azo Dyes. *Chem. Eng. J.* **2012**, *179*, 131−139.
(27) Zhao, Y. F.; Chen, P. Y.; Zhang, B. S.; Su, D. S.; Zhang, S. T.; Tian, L.; Lu, J.; Li, Z. X.; Cao, X. Z.; Wang, B. Y.; Wei, M.; Evans, D. G.; Duan, X. Highly Dispersed TiO_6 Units in a Layered Double Hydroxide for Water Splitting. *Chem.—Eur. J.* **2012**, *18*, 11949−11958.
(28) Moghaddam, H. K.; Pakizeh, M. Experimental Study on Mercury Ions Removal from Aqueous Solution by MnO_2/CNTs Nanocomposite Adsorbent. *J. Ind. Eng. Chem.* **2014**, DOI: 10.1016/j.jiec.2014.02.028.
(29) Foo, K. Y.; Hameed, B. H. Insights into the Modeling of Adsorption Isotherm Systems. *Chem. Eng. J.* **2010**, *156*, 2−10.
(30) Muhammad, M. J.; Ashiq, M. N. Adsorption of Dyes from Aqueous Solution on Activated Charcoal. *J. Hazard. Mater. B* **2007**, *139*, 57−66.
(31) Fan, L. L.; Luo, C. N.; Li, X. J.; Lu, F. G.; Qiu, H. M.; Sun, M. Fabrication of Novel Magnetic Chitosan Grafted with Graphene Oxide to Enhance Adsorption Properties for Methyl Blue. *J. Hazard. Mater.* **2012**, *215−216*, 272−279.
(32) Wu, T.; Cai, X.; Tan, S. Z.; Li, H. Y.; Liu, J. S.; Yang, W. D. Adsorption Characteristics of Acrylonitrile, p−Toluenesulfonic Acid, 1−Naphthalenesulfonic Acid and Methyl Blue on Graphene in Aqueous Solutions. *Chem. Eng. J.* **2011**, *173*, 144−149.
(33) Ai, L. H.; Yue, H. T.; Jiang, J. Sacrificial Template-Directed Synthesis of Mesoporous Manganese Oxide Architectures with Superior Performance for Organic Dye Adsorption. *Nanoscale* **2012**, *4*, 5401−5408.
(34) Velazquez-Jimenez, L. H.; Hurt, R. H.; Matos, J.; Rangel-Mendez, J. R. Zirconium−Carbon Hybrid Sorbent for Removal of Fluoride from Water: Oxalic Acid Mediated Zr (IV) Assembly and Adsorption Mechanism. *Environ. Sci. Technol.* **2014**, *48*, 1166−1174.
(35) Ma, J.; Yu, F.; Zhou, L.; Jin, L.; Yang, M. X.; Luan, J. S.; Tang, Y. H.; Fan, H. B.; Yuan, Z. W.; Chen, J. H. Enhanced Adsorptive Removal of Methyl Orange and Methylene Blue from Aqueous Solution by Alkali-Activated Multiwalled Carbon Nanotubes. *ACS Appl. Mater. Interfaces* **2012**, *4*, 5749−5760.
(36) Nayab, S.; Farrukh, A.; Oluz, Z.; Tuncel, E.; Tariq, S. R.; Rahman, H. U.; Kirchhoff, K.; Duran, H.; Yameen, B. Design and Fabrication of Branched Polyamine Functionalized Mesoporous Silica: An Efficient Absorbent for Water Remediation. *ACS Appl. Mater. Interfaces* **2014**, *6*, 4408−4417.

(37) Ghorai, S.; Sarkar, A.; Raoufi, M.; Panda, A. B.; Schönherr, H.; Pal, S. Enhanced Removal of Methylene Blue and Methyl Violet Dyes from Aqueous Solution Using a Nanocomposite of Hydrolyzed Polyacrylamide Grafted Xanthan Gum and Incorporated Nanosilica. *ACS Appl. Mater. Interfaces* **2014**, *6*, 4766−4777.
(38) Lian, G.; Zhang, X.; Si, H. B.; Wang, J.; Cui, D. L.; Wang, Q. L. Boron Nitride Ultrathin Fibrous Nanonets: One-Step Synthesis and Applications for Ultrafast Adsorption for Water Treatment and Selective Filtration of Nanoparticles. *ACS Appl. Mater. Interfaces* **2013**, *5*, 12773−12778.
(39) Jiang, W. J.; Cai, Q.; Xu, W.; Yang, M. W.; Cai, Y.; Dionysios, D. D.; O'Shea, K. E. Cr(VI) Adsorption and Reduction by Humic Acid Coated on Magnetite. *Environ. Sci. Technol.* **2014**, *48*, 8078−8085.
(40) Lim, Y. W. L.; Tang, Y. X.; Cheng, Y. H.; Chen, Z. Morphology, Crystal Structure and Adsorption Performance of Hydrothermally Synthesized Titania and Titanate Nanostructures. *Nanoscale* **2010**, *2*, 2751−2757.
(41) Zhou, J. B.; Tang, C.; Cheng, B.; Yu, J. G.; Jaroniec, M. Rattle-Type Carbon−Alumina Core−Shell Spheres: Synthesis and Application for Adsorption of Organic Dye. *ACS Appl. Mater. Interfaces* **2012**, *4*, 2174−2179.
(42) Ai, L. H.; Zhang, C. Y.; Meng, L. Y. Adsorption of Methyl Orange from Aqueous Solution on Hydrothermal Synthesized Mg−Al Layered Double Hydroxide. *J. Chem. Eng. Data* **2011**, *56*, 4217−4225.
(43) Goh, K.-H.; Lim, T.-T.; Dong, Z. L. Application of Layered Double Hydroxides for Removal of Oxyanions: A Review. *Water Res.* **2008**, *42*, 1343−1368.
(44) Gogoi, N.; Chowdhury, D. Novel Carbon Dot Coated Alginate Beads with Superior Stability, Swelling and pH Responsive Drug Delivery. *J. Mater. Chem. B* **2014**, *2*, 4089−4099.
(45) Ren, H.; Kulkarni, D. D.; Kodiyath, R.; Xu, W. N.; Choi, I.; Tsukruk, V. V. Competitive Adsorption of Dopamine and Rhodamine 6G on the Surface of Graphene Oxide. *ACS Appl. Mater. Interfaces* **2014**, *6*, 2459−2470.
(46) Ross, P. D.; Rekharsky, M. V. Thermodynamics of Hydrogen Bond and Hydrophobic Interactions in Cyclodextrin Complexes. *Biophys. J.* **1996**, *71*, 2144−2154.
(47) Cogoni, G.; Baratti, R.; Romagnoli, J. A. On the Influence of Hydrogen Bond Interactions in Isothermal and Nonisothermal Antisolvent Crystallization Processes. *Ind. Eng. Chem. Res.* **2013**, *52*, 9612−9619.
(48) Czeslik, C.; Jonas, J. Pressure and Temperature Dependence of Hydrogen-Bond Strength in Methanol Clusters. *Chem. Phys. Lett.* **1999**, *302*, 633−638.
(49) Li, J. Z.; Yao, K. D. Adsorption from Aqueous Solution Based on the Synergism between Hydrogen Bonding and Hydrophobic Interactions. *J. Appl. Polym. Sci.* **2005**, *96*, 841−845.
(50) Renault, F.; Morin-Crini, N.; Gimbert, F.; Badot, P.-M.; Crini, G. Cationized Starch-based Material as a New Ion-Exchanger Adsorbent for the Removal of C.I. Acid Blue 25 from Aqueous Solutions. *Bioresour. Technol.* **2008**, *99*, 7573−7586.